

A Mathematical Model for Copper Homeostasis in *Enterococcus hirae*

Elisabeth Pécou^{b,a,*} Alejandro Maass^{a,1} Daniel Remenik^a
Julien Briche^a Mauricio Gonzalez^{a,c,2}

^a*Laboratorio de Bioinformática y Matemática del Genoma, Centro de Modelamiento Matemático, U.M.I.-C.N.R.S. 2071, Av. Blanco Encalada 2120, Piso 7, Santiago, Chile*

^b*Institut de Mathématiques de Bourgogne, U.M.R. C.N.R.S. 5584, Université de Bourgogne, 9 Av. Alain Savary, BP 47870, 21078 Dijon Cedex, France.*

^c*Laboratorio de Bioinformática y Expresión Génica, INTA, Universidad de Chile, El Líbano 5524, Casilla 138-11, Santiago, Chile.*

Abstract

Copper is an essential micronutrient for life. It is required by a wide range of species, from bacteria to yeast, plants and mammals including humans. To prevent the consequences of the excess or deficit of copper, living organisms have developed molecular mechanisms that regulate the uptake, efflux, storage and use of the metal. However, the limits of homeostatic regulation are not known. Here, we take advantage of a simple biological mechanism involved in copper metabolism of *Enterococcus hirae*, to explore how the regulation is achieved by using a set of four proteins codified in the *cop* operon: two P-type ATP-ases copper transporters, one copper chaperon and one Cu-response transcription factor. We propose a mathematical model, based on differential equations and the power-law formalism (see *Savageau, M. A. (2001) Chaos 11(1), 142-159*), for the behavior of the *cop* operon and we show that homeostasis is a result of transient dynamics. The results derived from the mathematical model allow to measure qualitatively the adaptability of the system to its environment. This detailed model has been possible thanks to the available experimental biological information provided in a sequence of recent works by Solioz and co-workers.

Key words: Copper homeostasis, *cop* operon, *Enterococcus hirae*, systems biology, mathematical model, power-law formalism.

1 Introduction and Biological Background

Copper is a transition metal able to cycle between two redox states, oxidized Cu^{2+} and reduced Cu^{1+} , and it is an essential element in all biological systems. Its ability to accept and donate electrons gives copper the characteristic of being a very efficient cofactor in redox enzymes, but this reactivity nature of ionic copper also makes it a toxic metal (1; 2; 3). As a consequence, the cells must have mechanisms to handle properly the intracellular copper level (4). In the cell, copper homeostasis is controlled at three levels: (i) uptake, (ii) management and intracellular storage and (iii) copper efflux. Different bacterial proteins that bind to and/or transport copper are involved in this process (5). *E. hirae* is a broadly studied bacterial model for copper homeostasis. In this species, copper homeostasis is maintained by the *cop* operon, which is up-regulated by copper at concentrations higher than $10\ \mu\text{M}$ (6). The *cop* operon is formed by four genes *copA*, *copB*, *copY* and *copZ*, which encode two P-type ATP-ases copper transporters, a copper chaperon protein and a transcription factor that responds to copper, respectively. The copper ATPase CopA transports Cu^{1+} from extracellular to intracellular space in order to provide the copper requirements of the cell. In standard pH concentration, copper is available under the form of Cu^{2+} ions. Recently, the extracellular reductase CorA has been suspected to supply Cu^{1+} for uptake by CopA (6). Studies have shown that *E. hirae* mutants lacking the *copA* gene are able to grow like wild-type cells under conditions of normal or high extracellular copper levels, but also that, in a copper depleted medium, they cannot grow. This suggests that CopA ATPase is crucial for the copper import in limiting conditions of the metal (7). The CopA protein transfers the metal to CopZ, that exhibits a MxCxxC metal binding motif, characteristic of copper chaperons, and that binds one Cu^{1+} atom (8). It has been shown recently that the integrity of CopZ protein is modulated by the intracellular copper content. In fact, CopZ proteolysis was induced when bacteria were exposed to a high copper concentration (0.5 mM). This phenomenon has been observed in other proteins involved in copper metabolism (9). In vitro assays have shown that CopZ protein has the capacity to donate copper to the CopY repressor that binds to two Cu^{1+} atoms. The CopY is a Cu-response transcription factor that interacts with the promoter of *cop* operator and regulates the *cop* operon expression (6). In *E. hirae* growing under a limited extracellular copper availability, CopY binds to the promoter as a $(\text{Zn(II)CopY})_2$ complex and inhibits the *cop* operon expression. When extracellular copper concentration reaches $10\ \mu\text{M}$, the zinc atom is displaced by the Cu^{1+} donated by CopZCu or another

* Corresponding author. Phone: (56) (0)2 678 4525. Fax: (56) (0)2 688 9705.

Email address: epecou@u-bourgogne.fr (Elisabeth Pécou).

¹ Supported by the Nucleus Millennium Information and Randomness P001-05.

² Supported by grant FONDECYT 1030618.

intracellular Cu^{1+} complex (10). Then, CopY is released from the promoter, and the transcription of the *cop* operon proceeds (11). Despite the precise description of the mechanism controlling the activity of *cop* operon in *E. hirae*, the limits of homeostatic regulation are not known. Here, we take advantage of this description to provide a precise interpretation of such limits.

The approach of mathematical modelling to capture the role of regulation in biological systems is widely used, in particular to provide precise interpretations of non-intuitive data or to solve conflicts of biological hypotheses. In this article, we present a mathematical model describing the dynamical behavior of the components of the *cop* operon in *E. hirae*. The role of the *cop* operon is studied by simulating the proposed model in different extracellular copper concentrations. In this way, we estimate qualitatively the adaptability of the system to its environment. We do not use real parameters, since only few of them have been measured, but we consider qualitative relations among them and their order of magnitude. A program with a graphical interface was built to perform numerical simulations of the model.

The article is organized as follows. In Section 2, we propose a biological model for the behavior of *cop* operon, based on the available literature, and we explain the main simplifications made in our model. Sections 3 and 4 are devoted to the rigorous description of the mathematical model and its equations. In the case of a punctual source of external copper, we provide a theoretical proof of the existence of an equilibrium and its relation with homeostasis. Numerical simulations as well as the corresponding biological interpretation and discussion are given in Section 5 and Section 6 respectively. The software constructed to develop the numerical simulations is available at <http://www.cmm.uchile.cl/SBMLSim>.

2 The Biological Model: literature considerations

This section is mainly based on the experimental work of Solioz and co-workers ((6)-(8), (11)-(15)). We introduce some interpretations and simplifications of their data to isolate the dynamical behaviors we want to describe. The main simplification has to do with the consumption and storage of copper in the cell. We define a variable called *internal copper* to represent the copper not bound to a Cop protein. Evidence indicates that under normal conditions, it is virtually impossible to find free Cu ions inside the cell (4), and thus, this internal copper could be involved at the same time in storage and metabolic activities independent of the *cop* operon. However, the dynamics associated to the other internal copper uses introduces a complexity without changing the qualitative properties of regulation and homeostasis, which we show in the simplified *cop* operon model. Finally, in order to grasp the main features of

homeostasis, we focus the model only on the *cop* operon regulation of copper uptake and release.

2.1 The flow of copper

We use the following notations for Cop proteins that we illustrate in CopA: CopACu stands for the CopA protein bound to copper, CopA~ is a CopA protein free of copper. Moreover, CopA, CopA~ and CopACu stand at the same time for the entity and its concentration in the model. For example, we write: $\text{CopA} = \text{CopA}\sim + \text{CopACu}$. We describe hereafter the transit of copper ions inside the cell (see Figure 6, in Supplementary Information).

2.1.1 Uptake: CopA copper ATPase and other transporters

From biological experiments (15; 12), it has been proposed that the protein CopA is responsible of the copper uptake under extracellular copper limiting conditions. However, studies using *E. hirae* without the functional CopA protein indicate that the bacteria are able to grow in a medium supplemented with an excess of copper (6). This suggested that copper also enters into the cell in a passive way or through other cation transporters. We do not know how this transport occurs, but it seems to be necessary that the concentration of available copper overcomes a certain threshold in order to observe this alternative uptake. The uptake process is then described by the following reactions, where Cu_{ext} denotes the external source of copper and Cu_{int} denotes the internal concentration of copper not bound to any Cop protein:



2.1.2 Transfer of copper between CopA and CopZ.

Experimental evidence (12) shows that CopZ interacts with CopA and that this interaction is modulated by copper (the binding affinity is increased). On the other hand, when a complex CopA~CopZ containing copper dissociates, copper remains bound to CopZ (12). Thus, the copper flow is described by the following pair of reactions:

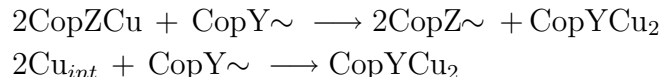


Multhaup et al (12) measured the kinetic parameters and they showed that they change in presence or absence of copper. In our model, the association rate of the first reaction is the rate measured when there is no available copper inside the cell ($2400M^{-1}s^{-1}$). The association rate and dissociation rate of the

second reaction are the values found in experiments with copper inside the cell ($2800M^{-1}s^{-1}$ and $10^{-3}s^{-1}$ respectively).

2.1.3 *Transfer of copper between CopZ and CopY.*

Two copper ions bind to each CopY molecule. CopY would receive copper either from CopZCu or from other Cu-complexes in the cell. Each complex CopZCu contains one copper ion. The reactions corresponding to these alternative ways of transferring copper to CopY are the following ones:



2.1.4 *The specificity in the pathway of copper transfer by CopZ*

It is not clear whether CopZ is devoted only to the transport of copper ions from CopA to CopY. In our model we include the possibility for CopZ or other copper chaperon proteins to deliver copper to the efflux pathway by transferring copper to CopB. In fact, in eukaryotic cells (from yeast to mammals) the copper efflux pathway involves a specific copper chaperon which delivers the metal to an ATPase efflux transporter like CopB ((16), (17)). In this context, it is reasonable to accept also the possibility that CopZ takes copper from complexes other than Cop proteins in the cell. This is reflected in our model by considering the capacity of CopZ to interact with internal copper.

2.1.5 *Copper efflux by CopB*

As was proposed, CopB may possibly accept copper from CopZ and/or other copper complexes. However, we do not know how many copper ions can bind to one protein CopB. The evidence shows that in other biological systems homologous CopB proteins can bind to two or more copper atoms (18): we denote this number by q . Even though, the mechanism of copper release by CopB is not completely clear. Our model assumes that this process can be activated when the bacterium reaches a sufficiently high internal copper concentration.

2.1.6 *Expelled copper*

We consider two situations:

- **Class I** systems: expelled copper is not available for the cells (at least for a while). In this case, we are assuming that the expelled copper leaves the system.

- **Class II** systems: expelled copper can be immediately (re)used by the cell.

2.1.7 Release of copper by degradation of Cop proteins

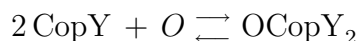
This is the last factor incorporated in the model for the transit of copper ions inside the cell. Following experimental data (4), we consider two a smaller degradation rate for CopZ \sim than for CopZCu. At this time there is no evidence of different degradation rates for the other Cop proteins.

2.2 Genetic regulation and genetic transcription of the cop operon

All four proteins are coded by the same operon (see Figure 7 in Supporting Information). We consider two possibilities:

- **Class A** systems: we include transcription and translation in one step. In this approach, we allow to include different speeds for each Cop protein. Considering that transcription and translation processes take longer times than those needed for the transit of copper among Cop proteins, we introduce a delay for the expression called T_e .
- **Class B** systems: we introduce mRNAs as variables of the system. Therefore transcription and translation are considered separately. In this case, we do not introduce time delays.

The role of CopY is to repress the transcription of the operon (negative feedback regulation). CopY interacts with two distinct sites of the promoter region of the *cop* operon in a homodimeric zinc protein form, acting as a copper-responsive repressor (13). When copper in the medium increases, two copper ions displace the zinc and cause the release of CopY from the DNA, allowing transcription (11). This is expressed in the following reaction:



The operon regulation mechanism is a simple negative feedback loop. When the copper inside the cell is low, this regulatory structure ensures the existence of a unique equilibrium state for concentrations of Cop proteins in the cell. The CopY protein has a negative control on its own transcription. Since CopY is inactivated by copper, regulation of the concentration of the Cop protein is tightly related to the copper concentration at each time. On the other hand, Cop proteins regulate the flow of copper inside the cell.

These facts suggest two hypotheses:

- (1) The fact that the proteins involved in the uptake and efflux of copper

are co-regulated indicates that the bacterium fits the dynamics of copper metabolism as a function of the extracellular copper concentration, which is variable at the time scale of the cell life.

- (2) Since that intracellular copper content depends on the transcriptional regulation of the *cop* operon, the bacterium will respond to variations in external copper concentrations in a transcriptional/translational time scale.

We explore these hypotheses in numerical experiments (see Section 5).

3 The Mathematical Modelling

In this section, we present a mathematical model for the system described in Section 2. We use the differential equations formalism. To justify this formalism all variables of the system have to evolve continuously and in a deterministic way. Since genetic entities and regulators are present in a low quantity in a cell, and this fact might imply stochastic effects, we assume that we are dealing with a population of cells and that our variables account for a mean behavior. This is a standard argument (see for instance (7)). Moreover, it is well adapted to experimental measurement results.

We also use polynomial equations (power-law formalism, (20)). Ultimately, this is always possible by enhancing the precision of the description, since at the scale of one chemical reaction the law of mass-action, which says that the speed of a reaction is proportional to the product of reactants concentrations, applies. In practice, some mechanisms are only partially known. When this occurs, we adapt the equations to fit the experimental observations. In our model, this happens for the copper uptake by a transporter different from CopA and the copper release by the CopB proteins. In this case, we use sigmoid shaped regulation functions. Both sigmoidal functions (alternative copper uptake \mathcal{R}_1 and efflux \mathcal{R}_2) have to satisfy, for $i=1,2$: (1) $\mathcal{R}_i(0) = 0$; (2) \mathcal{R}_i is small for concentrations lower than a threshold θ_i ; (3) \mathcal{R}_i grows proportionally to the concentration between θ_i and a second threshold θ'_i and (4) \mathcal{R}_i saturates for concentrations greater than θ'_i . We will consider essentially two types of functions : a non-linear sigmoidal function S_i and a piecewise linear function R_i (see Figures 8, 9 and 10 in Supporting Information).

3.1 Variables

The variables considered in the model are:

- The copper available in the medium at each time Cu_{ext} . We model an open system, that is, there exists an external source of copper which can enrich the medium at rate σ' .
- As we mentioned before (Section 2), the copper inside the cells Cu_{int} was introduced as a variable to represent the copper ions not bound to any Cop protein.
- We introduce variables for the concentration of all the Cop proteins (CopA, CopZ, CopY and CopB) and their parts bound to copper (CopACu, CopZCu, CopYCu₂ and CopBCu_q).
- To measure the level of activity of the transcription we introduce the variable OCopY_2 : the concentration of the *cop* operon containing the repressor CopY bound to the promoter region.

3.2 Parameters

The parameters considered are:

- The rate of external source of copper σ' is considered as an external parameter. We will take into account essentially two situations: (i) a point source of copper $\text{Cu}_{ext}(0) > 0$ together with $\sigma'(t) = 0$ for $t \geq 0$; and (ii) a constant rate of external source of copper $\sigma'(t) = s > 0$ for $t \geq 0$. The first one seems to be the more realistic in relation with the period of time under study.
- In Class A models, the operon parameters are the expression rates for CopA (respectively CopB, CopY and CopZ), denoted C_A (respectively C_B , C_Y and C_Z). The transcription-translation is proportional to the amount of free operon concentration, and its delay corresponds to T_e . In Class B models, the transcription rate for the mRNAs of CopA (respectively CopB, CopY and CopZ) is C'_A (respectively C'_B , C'_Y and C'_Z). Their transcription is proportional to the amount of free operon concentration. The translation rates are C_A (respectively C_B , C_Y and C_Z), and their translation is proportional to mRNAs' concentrations.
- Degradation rates of the Cop proteins: δ_A for CopA, δ_S for CopZ without copper and δ_Z for CopZCu, δ_Y for CopY and δ_B for CopB. In Class B models, we add degradation rates δ'_A , δ'_B , δ'_Y , and δ'_Z for the mRNAs.
- Affinity reactions constants: (1) copper uptake: k_A , k'_A ; (2) between Cop proteins: k_Z , k_Y , k_B ; (3) from internal copper to Cop proteins: cc_Y , cc_Z and cc_B ; (4) the reversible reaction of CopY with DNA: ρ_1 and ρ_2 ; and (5) the density of the *cop* operon regions ρ_0 . If the unit volume is the mean volume of one cell, then we can consider $\rho_0 = 1$.
- A positive integer q which represents the number of copper ions that can bind to a CopB protein.

3.3 The Mathematical Model

As stated before, we distinguish four versions of the model: Class AI (delay without recycling), Class AII (delay and recycling), Class BI (mRNA without recycling), and Class BII (mRNA and recycling). In this section, we present the system of ordinary differential equations corresponding to Class AI. The equations for the other classes of models are analogous and are presented in Figures 14, 15 and 16 of Supporting Information.

The reactions involved in the biological model are summarized in the scheme of Figure 11 and listed in Figure 12 in Supporting Information. All equations, except those corresponding to the copper uptake not mediated by CopA and efflux of copper are constructed according to a principle of mass conservation (see Figure 13, Supporting Information). Moreover, we assume that all reactions follow a mass action kinetics. To be coherent with the observed threshold phenomenon at the alternative copper uptake and the efflux, we use the regulation functions \mathcal{R}_1 and \mathcal{R}_2 . The equations for the systems of Class AI are presented right after (System Σ_{AI}). Notice that the dot over the variables means the time derivative. The following renaming of variables is used: $x_{11} = \text{Cu}_{ext}$, $x_1 = \text{Cu}_{int}$, $x_2 = \text{CopZCu}$, $x_3 = \text{CopYCu}_2$, $x_4 = \text{OCopY}_2$, $x_5 = \text{CopBCu}_q$, $x_6 = \text{CopACu}$, $x_7 = \text{CopA}$, $x_8 = \text{CopZ}$, $x_9 = \text{CopY}$, $x_{10} = \text{CopB}$.

$$\begin{aligned}
\dot{x}_{11} &= \sigma'(t) - k'_A \mathcal{R}_1(x_{11}) - k_A(x_7 - x_6)x_{11} \\
\dot{x}_1 &= k'_A \mathcal{R}_1(x_{11}) + \delta_A x_6 + q\delta_B x_5 + \delta_Z x_2 + 2\delta_Y x_3 - qcc_B x_1^q (x_{10} - x_5) \\
&\quad - 2cc_Y x_1^2 (x_9 - x_3) - cc_Z x_1 (x_8 - x_2) \\
\dot{x}_2 &= -\delta_Z x_2 + k_Z (x_8 - x_2)x_6 + cc_Z (x_8 - x_2)x_1 - 2k_Y (x_9 - x_3)x_2^2 \\
&\quad - qk_B (x_{10} - x_5)x_2^q \\
\dot{x}_3 &= -\delta_Y x_3 + k_Y (x_9 - x_3)x_2^2 + cc_Y (x_9 - x_3)x_1^2 \\
\dot{x}_4 &= -\rho_2 x_4 + \rho_1 (\rho_0 - x_4)(x_9 - x_3)^2 - \delta_Y x_4 \\
\dot{x}_5 &= -\delta_B x_5 - \tau \mathcal{R}_2(x_5) + k_B (x_{10} - x_5)x_2^q + cc_B (x_{10} - x_5)x_1^q \\
\dot{x}_6 &= -\delta_A x_6 + k_A (x_7 - x_6)x_{11} - k_Z (x_8 - x_2)x_6 \\
\dot{x}_7 &= C_A (\rho_0 - x_4(t - T_e)) - \delta_A x_7 \\
\dot{x}_8 &= C_Z (\rho_0 - x_4(t - T_e)) - \delta_Z x_2 - \delta_S (x_8 - x_2) \\
\dot{x}_9 &= C_Y (\rho_0 - x_4(t - T_e)) - \delta_Y x_9 + 2\rho_2 x_4 - 2\rho_1 (\rho_0 - x_4)(x_9 - x_3)^2 \\
\dot{x}_{10} &= C_B (\rho_0 - x_4(t - T_e)) - \delta_B x_{10}
\end{aligned}$$

4 Mathematical Analysis

In this section we present a rigorous analysis of the equilibrium state for the proposed model.

4.1 Analysis of stationary state: the case of a point source of copper

In this case $\sigma'(t) = 0$. We solve the equations for system *AI* (in System (AI)) with a nonlinear sigmoidal function for passive uptake and efflux.

One of the main reasons to present the complete analysis of this case is, first, because we can prove, independently of the values of parameters, the existence of a unique equilibrium state, and second, because in this simple case it is possible to describe homeostasis mathematically.

Now we proceed to analyze the equilibrium state of the system, that is, when the derivatives of the variables are equal to 0. From the first equation, we get Cu_{ext} is strictly decreasing. Then, $\text{Cu}_{ext} = 0$ at equilibrium.

Let C_{int} be the sum of all forms of internal copper, that is, $\text{Cu}_{int} + \text{CopZCu} + \text{CopYCu}_2 + \text{CopBCu}_q + \text{CopACu}$. By taking the derivative, observe that:

$$\dot{C}_{int} = k'_A \mathcal{R}_1(\text{Cu}_{ext}) - q\tau \mathcal{R}_2(\text{CopBCu}_q) + k_A \text{Cu}_{ext} \text{CopA}$$

This equality together with $\text{Cu}_{ext} = 0$ lead to $\mathcal{R}_2(\text{CopBCu}_q) = 0$, and thus $\text{CopBCu}_q = 0$ at equilibrium.

The equation $\text{CopBCu}_q = 0$ implies that either $\text{CopB} = 0$, or $\text{Cu}_{int} = \text{CopACu} = 0$. Suppose that $\text{CopB} = 0$, then by the equation $\text{CopB} = 0$, necessarily $\text{OCopY}_2 = \rho_0$. But this is incompatible with the equation $\text{OCopY}_2 = 0$ and the fact that $\rho_0 > 0$. The second possibility $\text{Cu}_{int} = \text{CopZCu} = 0$ implies through the equation $\text{Cu}_{int} = 0$ that $\text{CopYCu}_2 = \text{CopACu} = 0$.

Then we get $\text{CopA} = C_A/\delta_A(\rho_0 - \text{OCopY}_2)$, $\text{CopZ} = C_Z/\delta_S(\rho_0 - \text{CopZ})$ and $\text{CopB} = C_B/\delta_B(\rho_0 - \text{OCopY}_2)$ and the system:

$$\begin{cases} 0 = C_Y(\rho_0 - \text{OCopY}_2) - \delta_Y \text{CopY} + 2\rho_2 \text{OCopY}_2 \\ \quad - \rho_1(\rho_0 - \text{OCopY}_2) \text{CopY}^2 \\ 0 = -\rho_2 \text{OCopY}_2 + \rho_1(\rho_0 - \text{OCopY}_2) \text{CopY}^2 - \delta_Y \text{OCopY}_2 \end{cases} .$$

By substitution, we deduce that OCopY_2 is a zero of a polynomial function of degree three $P(x) = Ax^3 + Bx^2 + Cx + D = 0$ where $P(0) > 0$ ($D > 0$)

and $\lim_{x \rightarrow \infty} P(x) = -\infty$ ($A < 0$), then there always exists a real positive solution. Thus we have proven the existence of an equilibrium state. Without significant modifications the same result can be proven for systems in Class BI.

Numerical simulations in a large set of values for parameters suggest that this equilibrium is unique and stable. Also, for the other classes of systems and other sources of copper, numerical experiments suggest the existence of an equilibrium state.

4.2 *Mathematical homeostasis: circuits in the interaction graph*

In general, from a purely mathematical point of view, the homeostatic phenomenon is determined dynamically either by the existence of a stable equilibrium state or by the existence of an attracting periodic orbit with small amplitude oscillations. The nonlinearity of the biological networks under study makes very difficult to prove the existence of such attractive situations. The classical strategy consists in determining the existence of a negative feedback circuit in the interaction graph determined by the jacobian of the system of equations at each point (see the definition in (21)). It has been conjectured that such a circuit is a necessary condition for homeostasis (in the mathematical sense).

To be more precise, we write our system of equations as $\dot{x} = F(x)$ where $x = (x_1, \dots, x_n)$ is the vector of real variables and $F = (F_1, \dots, F_n)$ is the function of x determined by the right side of the system. Then the local interaction graph for this system at a point \bar{x} is obtained from the jacobian matrix of F at \bar{x} : its set of vertices is $\{1, \dots, n\}$ and there is an arrow oriented from a vertex i to a vertex j if and only if $\partial F_j / \partial x_i \neq 0$; this arrow is labelled with the sign of the partial derivative at \bar{x} . In Figure 1, a part of the interaction graph for a system in Class AI is shown. Notice that it does not depend on the parameters of the system except for the sign of the interaction from vertex representing OCopY_2 to vertex CopY .

In the simplified graph we can see a negative circuit (odd number of negative interactions) through Cu_{int} , CopY_{Cu} , OCopY_2 and CopB . This shows that the regulation of internal copper needs at least the activation of the operon and the efflux process. Observe that the only other possible negative circuit through Cu_{int} and OCopY_2 is that passing also through CopY when the undetermined arrow has a negative sign, and we do not know if this case happens. So, it is natural to ask whether the internal equilibrium can occur without the CopB protein.

4.3 Biological homeostasis

From a purely biological point of view homeostasis can have some additional flavors. In the case we are studying, homeostasis defines the ability of the bacterium to keep a certain level of internal copper to allow its normal growth, but preventing at the same time an excess of copper that becomes toxic. In other words, it is an adaptability condition, that is, the ability of the bacterium to move its internal state to a safe one, each time there is an external change in the copper conditions. This is a weak version of homeostasis, since it only requires to keep the value of the internal copper Cu_{int} (variable x_1) in some allowed interval $[\alpha, \beta]$, where β represents the level beyond which copper becomes toxic and α represents the minimum copper level necessary to satisfy the cell needs. Moreover, the property does not need to be verified at all times, but for an interval of time sufficiently large to allow division and growing of the bacterium.

Thus we define the *weak homeostasis condition* by:

$$\exists T > 0, \forall t \in [0, T], \alpha \leq x_1(t) \leq \beta. \quad (\text{WHC})$$

To examine the WHC for the system we consider the experimental condition given by a punctual external source of copper. Then, after a while, the biological system (or bacteria) is under copper limiting conditions. The main questions are: (i) *how long can it maintain the internal copper over some given α ?* and (ii) *according to its internal parameters, what concentration of internal copper is attained and for how long is the biological system able to maintain it under some given β ?*

Some preliminary results can be advanced from the rigorous mathematical result proved for models in Class AI (and Class BI), which say that the bacteria have a mechanism, that independently of their internal parameters, allows to move the system from any initial internal and external condition to an equilibrium state. The questions are, in view of the WHC, the time spent to arrive from such an external condition to an equilibrium and the values of the variables before and at the equilibrium. Without real values for the metabolic parameters it is difficult to state such bounds, but simulations show that the desired qualitative behavior occurs.

5 Results

The results of the numerical experiments presented in this section were made using a program specially built for this research. Nevertheless, the program was

developed in a generic way, in order to be adapted to other settings involving a differential equation model (SBMLSim, <http://www.dim.uchile.cl/SBML-Sim>).

The program is written in Matlab, and presents a graphical user interface that allows to change the parameters and initial conditions of the system, simulate it, and plot any expression of the variables. The specific model is constructed using the standard SBML (Systems Biology Markup Language, see <http://www.sbml.org>). The program translates the SBML file to several Matlab files that allow the simulation to run. In our case, the SBML files were generated using the software Cell Designer, <http://www.celldesigner.org>.

A well-known tool used to solve systems of differential equations and to visualize their solutions is XPPAUT, by G. Bard (<http://www.math.pitt.edu/bard/xpp/xpp.html>). The advantage of our simulator is that, while XPPAUT needs some knowledge of the user to handle the equations of the systems in order to work, our simulator is based on the automatic creation of the system of equations constructed via the SBML Toolbox, <http://sbml.org/software/sbmltoolbox>, starting from a SBML model file generated, for instance, by the Cell Designer software.

5.1 Typical behavior of the system

In this section, we describe the simulation of a system in Class BI, that is, without recycling and with mRNA, and we consider a point source of initial external copper. Since we do not dispose of precise parameters for the equations modelled before, we just consider reasonable relations between them. Also, in all the simulations the units are arbitrary. We set the parameters to the values presented in Table 1 in Supporting Information document. They have been chosen in order to follow generic relations described in the literature.

The typical trajectories of the most relevant quantities of the system between times $t = 0$ and $t = 2000$ are presented in Figure 2. The initial condition are the equilibrium values of the system starting with neither external nor internal copper. At initial time, none of the Cop proteins is bound to copper. Starting with that situation, we add a point source of copper $Cu_{ext}(0) = 50$. The four first pictures show the change of the amount of each Cop protein bound to copper (dash-dotted lines) and the amount of total Cop protein (solid lines). The qualitative behavior of the system is the following:

- **CopA** After adding the point source of copper, all available CopA \sim is transformed into CopACu. This quantity grows until the external source of copper is exhausted. Then, CopACu liberates the copper bound to it, and CopA \sim continues growing. After attaining a maximum it decreases to its

equilibrium value.

- **CopB** The trajectory of CopB starts just like the trajectory of CopA. When the intake of copper decreases, some CopBCu_q is transformed into CopB~. Unlike the CopA case, a fraction of CopB proteins remains as CopBCu_q. This quantity decreases a little, while CopB reaches a maximum and then both quantities (CopB and CopBCu_q) move in a rather similar way until reaching their equilibrium values, which are non-zero. This difference with the behavior of CopA (that persists for the other Cop proteins) is showing the fact that the only copper that binds to CopA is the external copper (so when the external copper is exhausted there is no more copper available for CopA), while the copper that stays into the cell continues to bind to CopB (and also to CopY and CopZ). It is interesting to remark that the total CopA and the total CopB attain their maxima at the same time (in fact, their trajectories are almost identical).
- **CopY** Once copper enters into the cell, all the available CopY, like CopA and CopB, is transformed into CopYCu₂ while there is available copper. In this case a high proportion of CopY is maintained in a CopYCu₂ form for a longer time than the other Cop proteins, including the moment when the total CopY attains its maximum. This behavior means that a very small fraction in the population of bacteria has its CopY bound to the *cop* operon, in the rest of the cells the transcription of the operon happens as fast as possible (see the plot for OCopY₂ in Figure 2). As the external copper source is depleted, there is an increment in the fraction of bacteria that change their content of CopYCu₂ into CopY which promote in these cells the binding of CopY to the operon. Thus, the transcription of genes encoded in the Cop operon (including CopY) starts to decrease until reaching a minimum, at this time both quantities (CopY and CopYCu₂) attain a relative equilibrium. Although, our results indicate that at equilibrium a major proportion of CopY continues in a CopYCu₂ form, the amount of CopYCu₂ appears to be not enough to sustain a level of transcription of the *cop* operon in order to support the increment of Cop proteins.
- **CopZ** Like in the previous cases, the copper that is incorporated binds to and exhausts the available CopZ. However, after this phase CopZCu decreases and CopZ changes its slope, exhibiting a different trajectory than the other Cop proteins. Probably the degradation rate of CopZCu, that is larger than the other three proteins with or without copper, implies that the total concentration of CopZ increases with a lower slope at the beginning. When the copper intake ceases, CopZCu goes to a lower level. The concentration of CopZ can be interpreted as a storage: when the external source of copper is depleted, CopZ continues to grow to a maximum level while CopZCu decreases to a very low level. If during this time there is another source of external copper, then there is a lot of CopZ to absorb the new requirements.
- **Internal free copper** Our simulation shows that the increment of the internal copper reaches its maximum before the external source of copper

has been depleted, supporting the ideas that copper forms a complex with the different Cop proteins present in the cell (including the new synthesized Cop proteins). The change in the slope may be associated to the contribution of the efflux process during the reduction of internal copper (observe that the minimum amount of internal copper is synchronized with the maximum amount of CopBCu₄). As the copper intake finishes, the rate of decreasing of the internal copper drastically changes and the remaining copper is expelled. The equilibrium attained is greater than zero because the bacteria require copper for metabolic activities independent of the *cop* operon, thus we expect that in this equilibrium there is no efflux.

- **CopY bound to the operon** The concentration of operon bound to CopY follows a trajectory quite different to that of CopYCu₂. This means that at the beginning, when a lot of copper is entering into the cell, the fraction of bacteria that change their content of CopY in CopYCu₂ increase until reaching a maximum. But when the internal copper approaches its equilibrium, the state of the system changes to start approaching the equilibrium of the other variables, which implies an increase of the concentration of operon occupied by CopY. This increment finishes at a value greater than the equilibrium, so a final decrease finishes by stabilizing the amount of free operon, thus determining a constant rate of transcription for further needs.

5.2 Differences between the models

We have introduced explicitly four classes of models (AI, AII, BI and BII).

We present here general results for each model and compare them with our basic case presented in Section 5.1 (Class AI model, see Figure 1716 in Supporting Information). In all the simulations we use an initial point source of external copper.

- **Class II Models** After a certain time, when copper efflux starts, the external copper rises until reaching its equilibrium value, which is greater than in Class I models, where external copper decrease monotonously. The system has the same sensitivity to a change in the parameters as Class BI models (see Section 5.4).
- **Class A-B Models** There is not a direct way to compare these models. The relationship between the delay and the affinity and velocity of the mRNA molecules is unknown, so only a qualitative comparison can be stated. In Figure 1817 in Supporting Information, we can notice a similar qualitative behaviour for both models in case of a small initial amount of copper. In the case of a little quantity of external copper the delay has quite the same incidence on the system as the degradation and the creation rate of mRNA. But for large values of the external copper the incidence differs. While for Class

B models the behavior changes when the mRNA parameters are changed, for Class A models the change of delays has no incidence. This accounts for the fact that if the external copper is too big, the CopY cannot stay bound to the operon for significant times, so in the equations, $\rho_0 - x_4$ can be considered to be ρ_0 , and as the delay participates only in x_4 (see System (Σ_{AI})), the delay has no significant incidence, as illustrated in Figure 1918, Supporting Information.

5.3 Some experiments related with different external sources of copper

The numerical experiments summarized in this section seek to understand the role played by the external source of copper in the dynamical behavior of the system.

The main conclusions drawn for a point source of copper are the following:

- Below a threshold the system does not extrude copper and above it some copper is expelled.
- The equilibrium attained inside the cell is constant for a sufficiently large source of copper, that is, from some point on, adding more external copper does not change the internal equilibrium, it only changes the trajectories to that equilibrium and the amount of copper expelled. As a consequence of this fact, it is observed that the relation between the amount of copper expelled and the size of the source is linear. Something similar happens for the maximum attained by the internal copper in the cell. In relation to the homeostasis this means that for sufficiently large values of the initial external source of copper, each extra unit of copper is translated into a fixed extra amount of the maximum attained by the internal copper.
- The time needed to attain the equilibrium depends on the size of the copper point source. For very low values of $Cu_{ext}(0)$, an increase in this value leads to a faster transcription of the *cop* operon and consequently to a faster achievement of the equilibrium. But for larger values of $Cu_{ext}(0)$ this phenomenon is overshadowed by the fact that more copper needs to be expelled, so that this efflux takes more time. We observe a logarithmic-like asymptotic increase for big values of $Cu_{ext}(0)$ (see Figure 3).
- In a copper shortage condition, CopA does take the role of transporting the scarce external copper into the cell, and in general it does not constitute a limiting factor.

The main conclusions drawn for a constant rate $\sigma' = s > 0$ of production of the external source of copper are:

- Figure 4 depicts the relations between the size of the source of copper with the equilibrium and with the maximum attained by the internal copper.

We observe that there is a critical value around $s = 1.95$ for this source. Below that threshold an equilibrium is attained, but it seems to appear an asymptotic behavior near the threshold: as the size of the constant source approaches the threshold, the equilibrium increases seemingly “ad infinitum”. Above that threshold, no equilibrium is attained and the internal copper grows indefinitely (at least for the scale of time that the simulator can handle).

- When the constant source of copper is suddenly removed, the system adjusts decreasing the transcription and a behavior similar to that observed for a punctual source of copper appears.

5.4 Ways to homeostasis

We are interested in the homeostasis phenomenon as defined in subsection 4.3.

5.4.1 Stable equilibrium

As we have seen, every model leads to an equilibrium in almost every situation (excepting the case when there is a big constant rate of production of external copper). The time needed for attaining the equilibrium depends on the initial values (as we saw in Section 5.3) and the value of the parameters.

In general, the time to equilibrium can be affected by making the *cop* operon “machinery” work faster. One way to do that is by rising the speed of the synthesis of the Cop proteins (in our case this corresponds in changing the parameters C_A , C_B , C_Y and C_Z and in the B case also C_{A2} , C_{B2} , C_{Y2} and C_{Z2}). See Figure 2019, Supporting Information.

5.4.2 Safe values of copper

As we have seen, the safety of the cell depends on having neither too much nor too few copper available. Notice that changing the parameters affects the amount of internal copper reached in the cell.

It is quite intuitive that the most relevant parameters for the maximum level of copper attained by the cell are those related with the intake. This is confirmed by the simulations (Figure 2120, Supporting Information). The maximum copper attained in the cell is also affected by the speed of the *cop* operon transcription: when the Cop proteins are created faster, the system is stabilized faster and consequently the maximum copper in the cell gets to a lower value. An interesting fact in this case is related to increasing only the velocity of transcription of CopA (Figure 2221, Supporting Information). One could

think that the this change would produce an increase in the equilibrium of the internal copper (as more CopA means a faster intake of copper). But the opposite happens.

The minimum level of copper needed by the cell must be respected by the equilibrium value of the internal copper. The most relevant parameters in this sense are the intake and efflux parameters. Changing the internal parameters also changes the equilibrium, but the effect is rather small (Figure 23, Supporting Information).

The general description of the dynamics shows that the *cop* operon provides an effective machinery to control the transfer, use and expulsion of copper from the cell, moving it to an equilibrium state after some transient dynamics. To attain its equilibrium state (that can be considered the normal state of the cell in absence of copper), the cell reaches a maximum which depends on parameters but also on the initial condition. This maximum can be toxic for the cell. So, from a purely mathematical point of view, adaptability can be interpreted as the capability of the cell to live within a reasonable initial condition of its variables in the model, in order to produce a safe maximum of free internal copper whenever the external source of copper changes.

6 Some final comments

The simulations (and rigorous mathematical proof for AI and BI models) confirm that the system attains an equilibrium, and that the machinery determined by the *cop* operon allows to adapt the internal state of the cell to changes in the external level of copper. Part of the copper that enters into the cell leaves it, and (generally a smaller) part stays inside the cell, both as internal copper (in our model) and as copper bound to Cop proteins. The only situations where an equilibrium is not attained and the amount of internal free copper explodes is when there is a large and constant source of external copper. In Figure 5 a cycle constituted by three impulses of external copper is shown. After the first impulse the cell is adapted for the future resistance to the metal.

Even if not all the genome components involved in copper metabolism are known, the introduction of the internal copper variable allows to evaluate this metabolism only looking to the *cop* operon. Moreover, it also allows to establish which elements of the operon are more relevant for copper metabolism and its homeostasis.

Finally, let us notice that besides the interpretation of the homeostatic machinery, the model also allows to study the effect of *cop* operon operation in

the cellular population.

Acknowledgment. We thank Angélica Reyes for valuable discussions and critical reading of the manuscript.

References

- [1] M.C. Linder, M. Hazegh-Azam, Copper biochemistry and molecular biology. *Am. J. Clin. Nutr.* 63 (1996) 797-811.
- [2] R.R. Crichton, J.L. Pierre, Old iron, young copper: from Mars to Venus. *Biometals* 14 (2001) 99-112.
- [3] N.K. Urbanski, A. Beresewicz, Generation of *OH initiated by interaction of Fe²⁺ and Cu⁺ with dioxygen; comparison with the Fenton chemistry. *Acta Biochim. Pol.* 47 (2000) 951-962.
- [4] T. Rae, P.J. Schmidt, R.A. Pufahl, V.C. Culotta, T.V. O'Halloran, Undetectable intracellular free copper: the requirement of a copper chaperone for superoxide dismutase. *Science* 284 (1999) 805-808.
- [5] N. Nelson, Metal ion transporters and homeostasis. *EMBO J.* 18 (1999) 4361-4371.
- [6] M. Solioz, J.V. Stoyanov, Copper homeostasis in *Enterococcus hirae*. *FEMS Microbiology Reviews* 27 (2003) 183-195.
- [7] A. Odermatt, H. Sutert, R. Krapfs, M. Solioz, Primary structure of two P-type ATPases involved in copper homeostasis in *Enterococcus hirae*. *J. Biol Chem.* 268 (1993) 12775-12779.
- [8] Z. Lu, M. Solioz, Copper-induced proteolysis of the CopZ copper chaperone of *Enterococcus hirae*. *J. Biol Chem.* 276 (2001) 47822-47827.
- [9] M.J. Petris, K. Smith, J. Lee, D.J. Thiele, Copper-stimulated endocytosis and degradation of the human copper transporter, hCtr1. *J. Biol. Chem.* 278 (2003) 9639-9646.
- [10] P. Cobine, W.A. Wickramasinghe, M.D. Harrison, T. Weber, M. Solioz, C.T. Dameron, The *Enterococcus hirae* copper chaperone CopZ delivers copper(I) to the CopY repressor. *FEBS Lett.* 445 (1999) 27-30.
- [11] P. Cobine, G.N. George, C. Jones, W. Wickramasinghe, M. Solioz, C. Dameron, Copper transfer from the Cu(I) chaperone, CopZ, to the repressor, Zn(II)CopY: metal coordination environments and protein interactions. *Biochemistry* 41 (2002) 5822-5829.
- [12] G. Multhaup, D. Strausak, K.D. Bissig, M. Solioz, Interaction of the CopZ copper chaperone with the CopA copper ATPase of *Enterococcus hirae* assessed by surface plasmon resonance. *Biochem. Biophys. Res. Commun.* 288 (2001) 172-177.
- [13] R. Portmann, D. Magnani, J.V. Stoyanov, A. Schmechel, G. Multhaup, M. Solioz, Interaction kinetics of the copper-responsive CopY repressor

- with the cop promoter of *Enterococcus hirae*. *J. Biol. Inorg. Chem.* 9 (2004) 396-402.
- [14] M. Solioz, A. Odermatt, Copper and silver transport by CopB-ATPase in membrane vesicles of *Enterococcus hirae*. *J Biol Chem.* 270 (1995) 9217-9221.
- [15] H. Wunderli-Ye, M. Solioz, Purification and functional analysis of the copper ATPase CopA of *Enterococcus hirae*. *Biochem. Biophys. Res. Commun.* 280 (2001) 713-719.
- [16] R.A. Pufahl, C.P. Singer, K.L. Peariso, S.J. Lin, P.J. Schmidt, C.J. Fahrni, V.C. Culotta, J.E. Penner-Hahn, T.V. O'Halloran, Metal ion chaperone function of the soluble Cu(I) receptor Atx1. *Science.* 278 (1997) 853-856.
- [17] D. Strausak, M.K. Howie, S.D. Firth, A. Schlicksupp, R. Pipkorn, G. Multhaup, J.F. Mercer, Kinetic analysis of the interaction of the copper chaperone Atox1 with the metal binding sites of the Menkes protein. *J Biol Chem* 278 (2003) 20821-20827.
- [18] S. Lutsenko, K. Petrukhin, M.J. Cooper, C. Gilliam, J.H. Kaplan, N-terminal domains of human copper-transporting adenosine triphosphatases (the Wilson's and Menkes disease proteins) bind copper selectively in vivo and in vitro with stoichiometry of one copper per metal-binding repeat. *J. Biol. Chem.* 272 (1997) 18939-18944.
- [19] H. Othmer, The qualitative dynamics of a class of biochemical control circuits. *J. Math. Biol.* 3 (1) (1976) 53-78.
- [20] M.A. Savageau, Design principles for elementary gene circuits: Elements, methods, and examples. *Chaos* 11(1) (2001) 142-159.
- [21] C. Soulé, Graphic requirements for multistability, *ComplexUs* 1 (2003) 123-133.
- [22] Kohn KW. *Chaos* 11 (2001) 84-97.

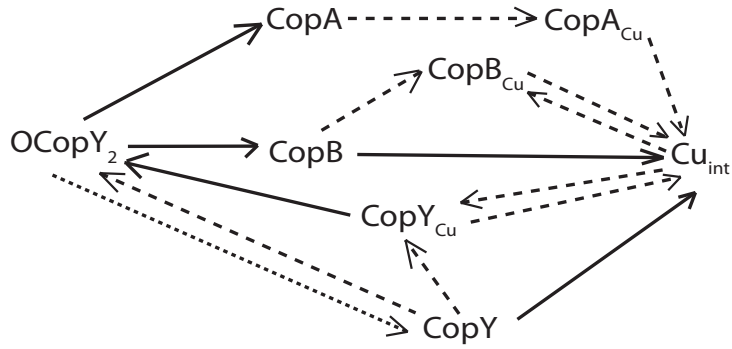


Fig. 1. The interaction graph associated to system *AI* without CopZ variables and auto-feedback inhibition. Solid arrows represent negative interactions whereas dashed arrows represent positive interactions. The sign of the arrow between $OCopY_2$ and CopY is undetermined.

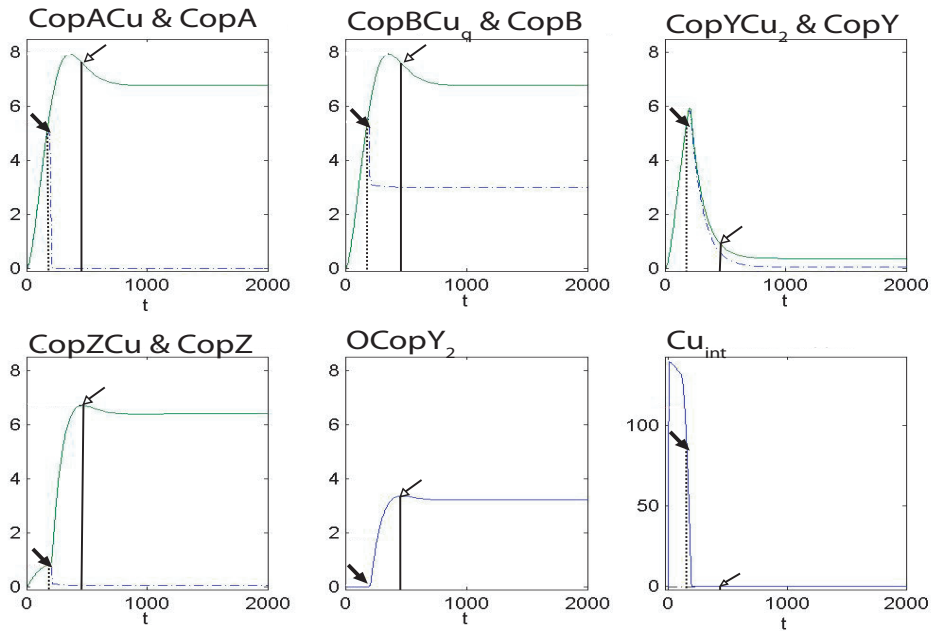


Fig. 2. Trajectories of the most relevant variables of the system when there is a point source of copper $Cu_{ext}(0) = 50$. The external copper is exhausted by a time around $t = 230$ (black solid arrow). The empty arrow indicates the maximum state of repression of the operon (maximum of $OCopY_2$). The CopY picture does not consider the portion of the protein bound to the promoter region.

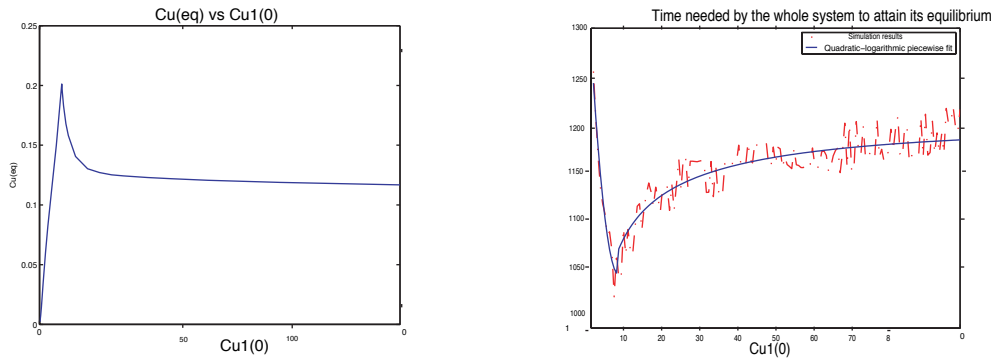


Fig. 3. Relation of the equilibrium attained by the internal copper and the time to equilibrium with a point source of external copper.

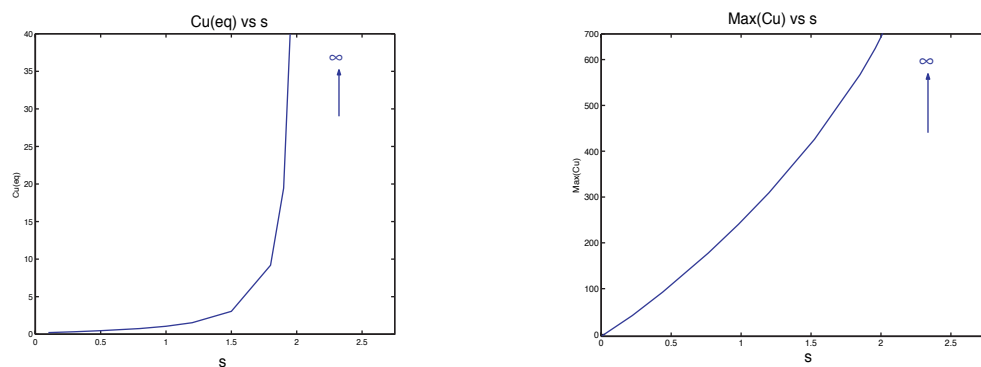


Fig. 4. The equilibrium and the maximum of the internal free copper as functions of $\sigma' = s$. For values greater than a threshold around the internal free copper grows indefinitely.

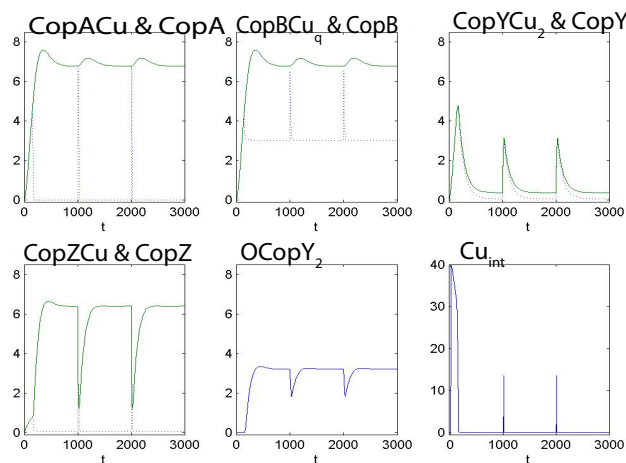


Fig. 5. The figure depicts the dynamics of the system for three different punctual sources of external copper, each one after a local equilibrium.

7 Supplementary Information

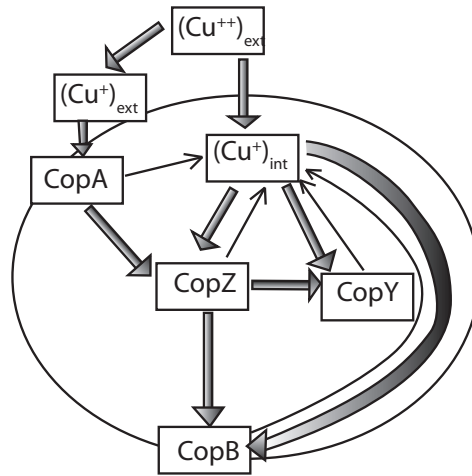


Fig. 6. The transit of copper inside the cell. Thick arrows mean transport of copper and thin arrows represent degradation.

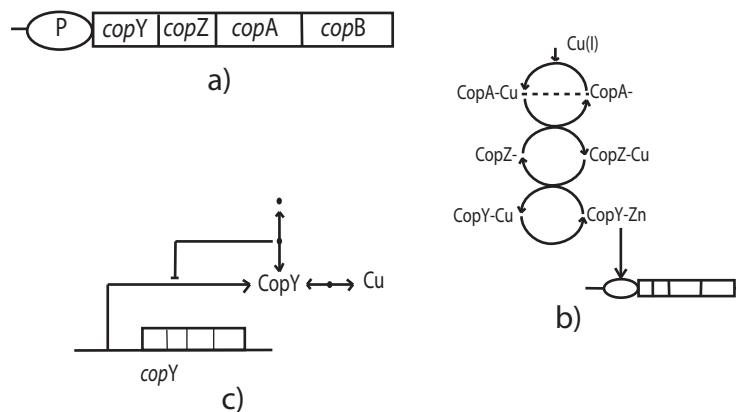


Fig. 7. (a) The Cop operon has a promoter region P and it is composed of four genes: *copY*, *copZ*, *copA* and *copB*. (b) The input signal for the *cop* operon: extracellular copper. Copper binds to the receptor protein CopA transporter. After a short pathway of copper transfer involving CopZ, copper binds to the regulator protein CopY. (c) The regulation mechanism depicted following Kohn's graphical formalism (22). The protein CopY transcribed from *copY* either binds to a copper ion or forms a homodimer (13) that binds to the promoter region P and stops the transcription.

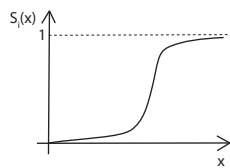


Fig. 8. Sigmoidal regulation function $S_i = \frac{1+x^{p_i}}{K_i+x^{p_i}} - \frac{1}{K_i}$, where $p_i > 1$ and $K_i > 1$.

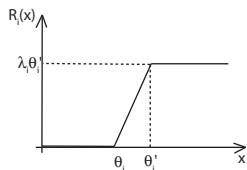


Fig. 9. Piecewise-linear regulation function $R_i = \max(0, \min(\lambda_i(x - \theta_i), \lambda_i(\theta_i' - \theta_i)))$.

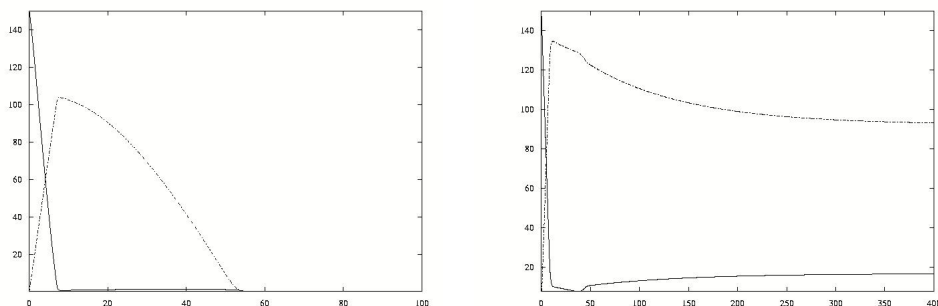


Fig. 10. In the simulations, we consider two classes of models, **Class S** and **Class R**, according to the choice of regulation function (nonlinear sigmoidal and piecewise linear, respectively). The main difference between the two classes is that while in class R models there are thresholds that avoid the intake and efflux of copper before certain critical values, in class S models the function only tends toward 0 for little values, so there is always a residual exchange between inside and outside the cell. This difference is noticed in the simulations results in this picture. Indeed, the results show us that in the S case the internal and the external copper go to 0, while in the R case there is always a certain quantity of copper left inside the cell (the external copper always goes to 0 because CopA is always able to take it into the cell). For all other numerical experiments that have been driven, only minor differences have been noticed. *Left*: Trajectories of the internal (dashed line) and external (continuous line) copper in class AIS. The values at equilibrium tend toward 0, even if there is recycling. *Right*: Trajectories of the internal (dashed line) and external (continuous line) copper in class AIR. The equilibrium values are greater than 0. (In both plots $Cu_{\text{ext}}(0) = 150$).

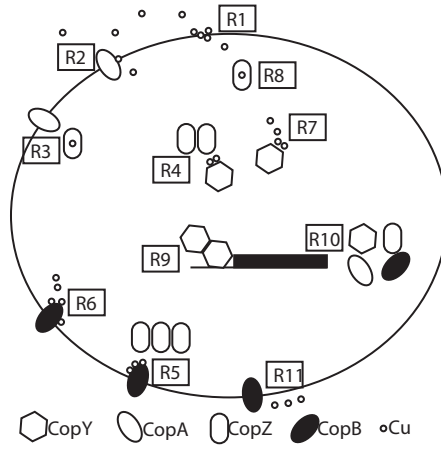


Fig. 11. Global view of all the reactions (we have omitted degradation reactions)

R1	$\text{Cu}_{\text{ext}} \longrightarrow \text{Cu}_{\text{int}}$	R1	$v_1 = k_1 \mathcal{R}_1(\text{Cu}_{\text{ext}})$	
R2	$\text{Cu}_{\text{ext}} + \text{CopA} \sim \longrightarrow \text{CopACu}$	R2	$v_2 = k_2(\text{CopA} \sim)(\text{Cu}_{\text{ext}})$	
R3	$\text{CopACu} + \text{CopZ} \sim \longrightarrow \text{CopA} \sim + \text{CopZCu}$	R3	$v_3 = k_3(\text{CopACu})(\text{CopZ} \sim)$	
R4	$2\text{CopZCu} + \text{CopY} \sim \longrightarrow 2\text{CopZ} \sim + \text{CopYCu}_2$	R4	$v_4 = k_4(\text{CopZCu})^2(\text{CopY} \sim)$	
R5	$q\text{CopZCu} + \text{CopB} \sim \longrightarrow q\text{CopZ} \sim + \text{CopBCu}_q$	R5	$v_5 = k_5(\text{CopZCu})^q(\text{CopB} \sim)$	
R6	$q\text{Cu}_{\text{int}} + \text{CopB} \sim \longrightarrow \text{CopBCu}_q$	R6	$v_6 = c c_q(\text{Cu}_{\text{int}})^q(\text{CopB} \sim)$	
R7	$2\text{Cu}_{\text{int}} + \text{CopY} \sim \longrightarrow \text{CopYCu}_2$	R7	$v_7 = c c_2(\text{Cu}_{\text{int}})^2(\text{CopY} \sim)$	
R8	$\text{Cu}_{\text{int}} + \text{CopZ} \sim \longrightarrow \text{CopZCu}$	R8	$v_8 = c c_1(\text{Cu}_{\text{int}})(\text{CopZ} \sim)$	
R9	$\text{O} + 2\text{CopY} \sim \rightleftharpoons \text{OCopY}_2$	R9	$v_9 = \rho_1(\text{O})(\text{CopY} \sim)^2 \quad v_{10} = \rho_2(\text{OCopY}_2)$	
R10 _A	$\text{O} \longrightarrow \text{O} + \text{CopA} \sim$	R10 _B	$\text{O} \longrightarrow \text{O} + \text{CopB} \sim$	
R10 _Y	$\text{O} \longrightarrow \text{O} + \text{CopY} \sim$	R10 _Z	$\text{O} \longrightarrow \text{O} + \text{CopZ} \sim$	
R11	$\text{CopBCu}_q \longrightarrow q(\text{Cu}_{\text{ext}})^* + \text{CopB} \sim$		R11	$v_{11} = \tau \mathcal{R}_1(\text{CopBCu}_q)$
R12 _A	$\text{CopA} \sim \longrightarrow \bullet$	R12 _A [']	$\text{CopACu} \longrightarrow \bullet + \text{Cu}_{\text{int}}$	
R12 _B	$\text{CopB} \sim \longrightarrow \bullet$	R12 _B [']	$\text{CopBCu}_q \longrightarrow \bullet + q\text{Cu}_{\text{int}}$	
R12 _Z	$\text{CopZ} \sim \longrightarrow \bullet$	R12 _Z [']	$\text{CopZCu} \longrightarrow \bullet + \text{Cu}_{\text{int}}$	
R12 _Y	$\text{CopY} \sim \longrightarrow \bullet$	R12 _Y [']	$\text{CopYCu}_2 \longrightarrow \bullet + 2\text{Cu}_{\text{int}}$	
R12 _Y ^{''}	$\text{OCopY}_2 \longrightarrow \bullet + \text{O}$		R12 _Y ^{''}	$v_{12Y}^{\prime\prime} = \delta_1(\text{OCopY}_2)$
			R12 _A	$v_{12A} = \delta_2(\text{CopA} \sim)$
			R12 _A [']	$v_{12A}^{\prime} = \delta_3(\text{CopACu})$
			R12 _Y ^{''}	$v_{12Y}^{\prime\prime} = \delta_4(\text{OCopY}_2)$

Fig. 12. List of all the reactions and their rates in Class A models.

$$(\Sigma_{AI}) \left\{ \begin{array}{l}
\dot{C}u_{ext} = \sigma'(t) - v_1 - v_2 \\
\dot{C}u_{int} = v_1 + v'_{12A} + qv'_{12B} + 2v'_{12Y} + v'_{12Z} - qv_6 - 2v_7 - v_8 \\
\text{Cop}\dot{A}Cu = v_2 - v_3 - v'_{12A} \\
\text{Cop}\dot{Z}Cu = v_3 + v_8 - 2v_4 - qv_5 - v'_{12Z} \\
\text{Cop}\dot{Y}Cu_2 = v_4 + v_7 - v'_{12Y} \\
\text{Cop}\dot{B}Cu_q = v_5 + v_6 - v_{11} - v'_{12B} \\
\text{OCop}\dot{Y}_2 = v_9 - v'_9 - v''_{12Y} \\
\text{Cop}\dot{A} = -v_{12A} - v'_{12A} + v_{10A} \\
\text{Cop}\dot{Z} = -v_{12Z} - v'_{12Z} + v_{10Z} \\
\text{Cop}\dot{Y} = -v_{12Y} - v'_{12Y} + v_{10Y} - 2v_9 + 2v'_9 \\
\text{Cop}\dot{B} = -v_{12B} - v'_{12B} + v_{10B}
\end{array} \right.$$

Fig. 13. The equations for the Class AI systems.

R13 _A	$O \longrightarrow \text{mRNA}_A + O$	R13 _B	$O \longrightarrow \text{mRNA}_B + O$
R13 _Y	$O \longrightarrow \text{mRNA}_Y + O$	R13 _Z	$O \longrightarrow \text{mRNA}_Z + O$
R14 _A	$\text{mRNA}_A \longrightarrow \text{CopA}\sim + \text{mRNA}_A$	R14 _B	$\text{mRNA}_B \longrightarrow \text{CopB}\sim + \text{mRNA}_B$
R14 _Y	$\text{mRNA}_Y \longrightarrow \text{CopY}\sim + \text{mRNA}_Y$	R14 _Z	$\text{mRNA}_Z \longrightarrow \text{CopZ}\sim + \text{mRNA}_Z$
R15 _A	$\text{mRNA}_A \longrightarrow \bullet$	R15 _B	$\text{mRNA}_B \longrightarrow \bullet$
R15 _Y	$\text{mRNA}_Y \longrightarrow \bullet$	R15 _Z	$\text{mRNA}_Z \longrightarrow \bullet$

R13 _A	$\mathbf{v}_{13A} = C_A'(O)$	R13 _B	$\mathbf{v}_{13B} = C_B'(O)$
R13 _Y	$\mathbf{v}_{13Y} = C_Y'(O)$	R13 _Z	$\mathbf{v}_{13Z} = C_Z'(O)$
R14 _A	$\mathbf{v}_{14A} = C_A(\text{mRNA}_A)$	R14 _B	$\mathbf{v}_{14B} = C_B(\text{mRNA}_B)$
R14 _Y	$\mathbf{v}_{14Y} = C_Y(\text{mRNA}_Y)$	R14 _Z	$\mathbf{v}_{14Z} = C_Z(\text{mRNA}_Z)$
R15 _A	$\mathbf{v}_{15A} = \delta_A'(\text{mRNA}_A)$	R15 _B	$\mathbf{v}_{15B} = \delta_B'(\text{mRNA}_B)$
R15 _Y	$\mathbf{v}_{15Y} = \delta_Y'(\text{mRNA}_Y)$	R15 _Z	$\mathbf{v}_{15Z} = \delta_Z'(\text{mRNA}_Z)$

Fig. 14. List of the supplementary reactions and their rates in Class B models.

$$(\Sigma_{BI}) \left\{ \begin{array}{l}
\dot{C}u_{ext} = \sigma'(t) - v_1 - v_2 \\
\dot{C}u_{int} = v_1 + v'_{12A} + qv'_{12B} + 2v'_{12Y} + v'_{12Z} - qv_6 - 2v_7 - v_8 \\
\text{Cop}\dot{A}Cu = v_2 - v_3 - v'_{12A} \\
\text{Cop}\dot{Z}Cu = v_3 + v_8 - 2v_4 - qv_5 - v'_{12Z} \\
\text{Cop}\dot{Y}Cu_2 = v_4 + v_7 - v'_{12Y} \\
\text{Cop}\dot{B}Cu_q = v_5 + v_6 - v_{11} - v'_{12B} \\
O\text{Cop}\dot{Y}_2 = v_9 - v'_9 - v''_{12Y} \\
mR\dot{N}A_A = v_{13A} - v_{15A} \\
mR\dot{N}A_A = v_{13Z} - v_{15Z} \\
mR\dot{N}A_A = v_{13Y} - v_{15Y} \\
mR\dot{N}A_A = v_{13B} - v_{15B} \\
\text{Cop}\dot{A} = -v_{12A} - v'_{12A} + v_{14A} \\
\text{Cop}\dot{Z} = -v_{12Z} - v'_{12Z} + v_{14Z} \\
\text{Cop}\dot{Y} = -v_{12Y} - v'_{12Y} + v_{14Y} - 2v_9 + 2v'_9 \\
\text{Cop}\dot{B} = -v_{12B} - v'_{12B} + v_{14B}
\end{array} \right.$$

Fig. 15. The equations for the Class BI systems.

$$(\Sigma_{BI}) \left\{ \begin{array}{l}
\dot{x}_{11} = \sigma'(t) - k'_A \mathcal{R}_1(x_{11}) - k_A(x_7 - x_6)x_{11} \\
\dot{x}_1 = k'_A \mathcal{R}_1(x_{11}) + \delta_A x_6 + q\delta_B x_5 + \delta_Z x_2 + 2\delta_Y x_3 - qcc_B x_1^q (x_{10} - x_5) \\
\quad - 2cc_Y x_1^2 (x_9 - x_3) - cc_Z x_1 (x_8 - x_2) \\
\dot{x}_2 = -\delta_Z x_2 + k_Z (x_8 - x_2)x_6 + cc_Z (x_8 - x_2)x_1 - 2k_Y (x_9 - x_3)x_2^2 \\
\quad - qk_B (x_{10} - x_5)x_2^q \\
\dot{x}_3 = -\delta_Y x_3 + k_Y (x_9 - x_3)x_2^2 + cc_Y (x_9 - x_3)x_1^2 \\
\dot{x}_4 = -\rho_2 x_4 + \rho_1(\rho_0 - x_4)(x_9 - x_3)^2 - \delta_Y x_4 \\
\dot{x}_5 = -\delta_B x_5 - \tau \mathcal{R}_2(x_5) + k_B (x_{10} - x_5)x_2^q + cc_B (x_{10} - x_5)x_1^q \\
\dot{x}_6 = -\delta_A x_6 + k_A (x_7 - x_6)x_{11} - k_Z (x_8 - x_2)x_6 \\
\dot{y}_7 = C'_A (\rho_0 - x_4) - \delta'_A y_7 \\
\dot{x}_7 = C_A y_7 - \delta_A x_7 \\
\dot{y}_8 = C'_Z (\rho_0 - x_4) - \delta'_Z y_8 \\
\dot{x}_8 = C_Z y_8 - \delta_Z x_2 - \delta_S (x_8 - x_2) \\
\dot{y}_9 = C'_Y (\rho_0 - x_4) - \delta'_Y y_9 \\
\dot{x}_9 = C_Y y_9 - \delta_Y x_9 + 2\rho_2 x_4 - 2\rho_1(\rho_0 - x_4)(x_9 - x_3)^2 \\
\dot{y}_{10} = C'_B (\rho_0 - x_4) - \delta'_B y_{10} \\
\dot{x}_{10} = C_B y_{10} - \delta_B x_{10}
\end{array} \right.$$

Fig. 16. The equations for the Class BI systems using the renaming of the variables.

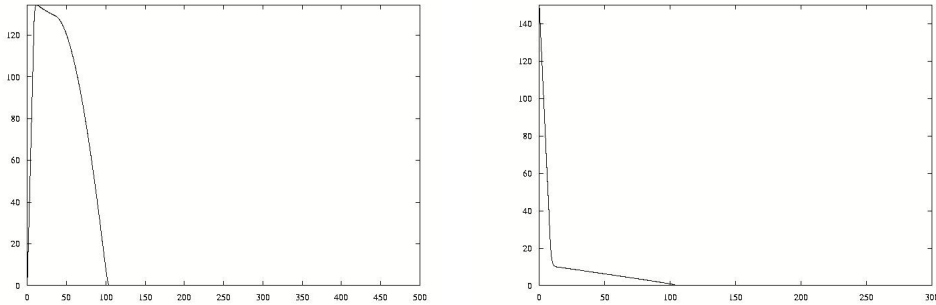


Fig. 17. The trajectories of the internal (left) and external (right) copper for models in class AIR.

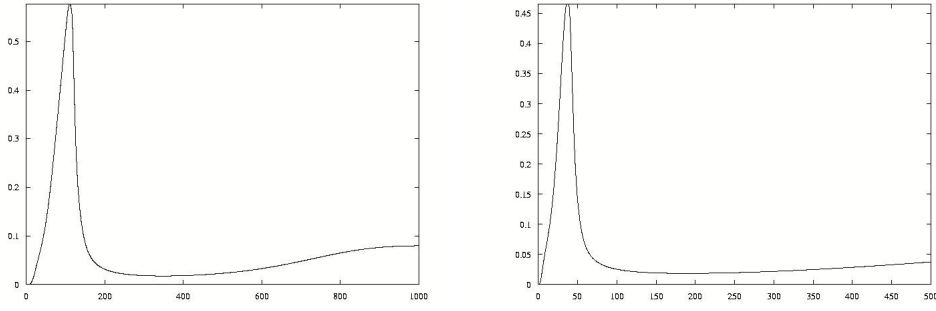


Fig. 18. Trajectory of the internal copper in class BIR (left) and in class AIR (right) for an initial point source of copper $Cu_{\text{ext}}(0) = 10$.

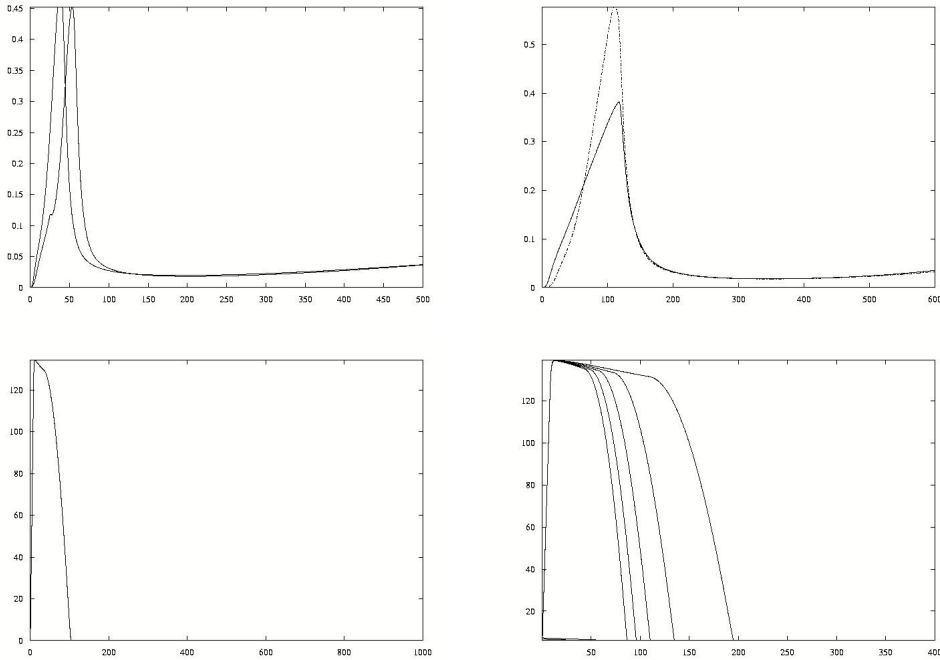


Fig. 19. *Left-up*: Trajectory (for $Cu_{\text{ext}}(0) = 10$) of the internal free copper in class AIR for different values of the delay. For larger values of the delay, the system spends more time to reach the equilibrium. *Right-up*: Trajectory (for $Cu_{\text{ext}}(0) = 10$) of the internal copper in class BIR for different values of parameter δ_A . When δ_A grows, the maximum of the copper in the cell decreases. *Left-down*: Trajectory (for $Cu_{\text{ext}}(0) = 150$) of the internal copper in class AIR for different values of the delay. No significant difference is made by the change in the delay. *Right-down*: Trajectory (for $Cu_{\text{ext}}(0) = 150$) of the internal copper in class BIR for different values C_{B2} , the rate of transcription of mRNA_B . When C_{B2} grows, the time to reach the equilibrium decreases.

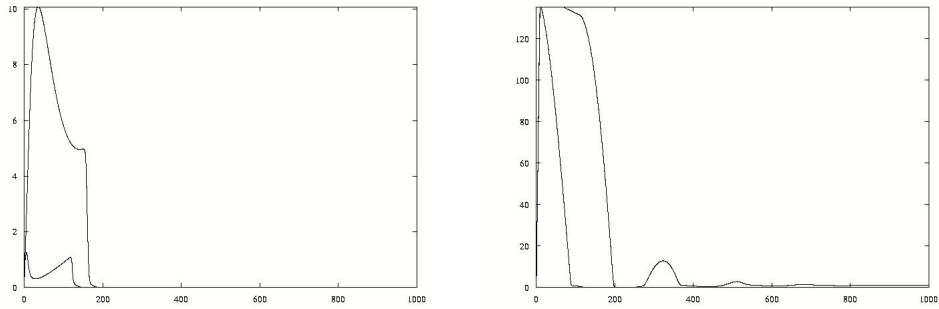


Fig. 20. *Left:* Trajectory of the internal copper in class AIIS for different values of C_B . The increase of C_B produces a decrease in the time to equilibrium. *Right:* Trajectory of the internal copper in class BIIR for different values of C_{Y_2} . The increase of C_{Y_2} produces a decrease in the time to equilibrium and, in this case, some oscillations become visible. In both plots $Cu_{\text{ext}}(0) = 150$.

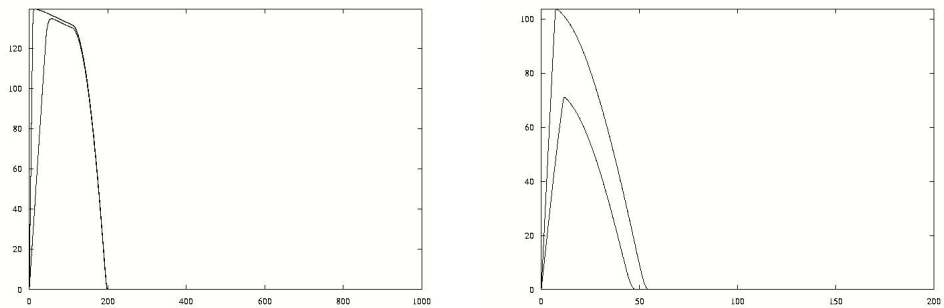


Fig. 21. *Left:* Trajectory of the internal copper in class BIIR for different values of k'_A , the rate of direct diffusion of copper into the cell. Increasing k'_A produces a lower and later maximum of the internal copper. *Right:* Trajectory of the internal copper in class AIS for different values of k_1 . Increasing k_1 produces a decrease in the time needed to attain the equilibrium and the maximum attained by the internal free copper.

—abelf.21

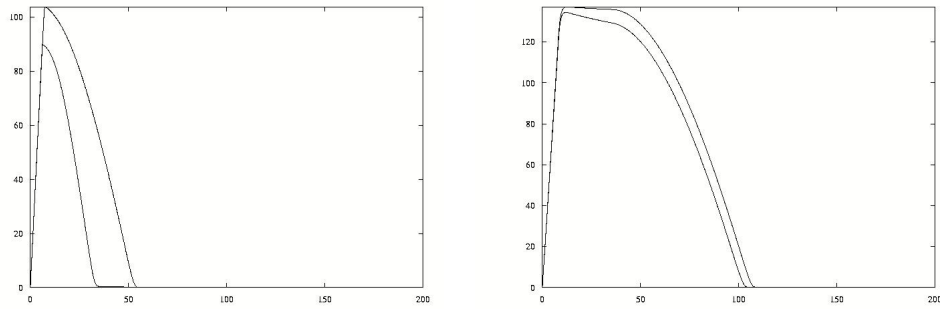


Fig. 22. *Left:* Trajectory of the internal free copper in class AIS for different values of C_A . Increasing C_A produces a decrease in the time needed to attain the equilibrium and the maximum attained by the internal free copper. *Right:* Trajectory of the internal free copper in class AIIR for different values of δ_Z . Increasing δ_Z produces an increase in the time needed to attain the equilibrium and the maximum attained by the internal copper. In both plots $Cu_{\text{ext}}(0) = 150$.

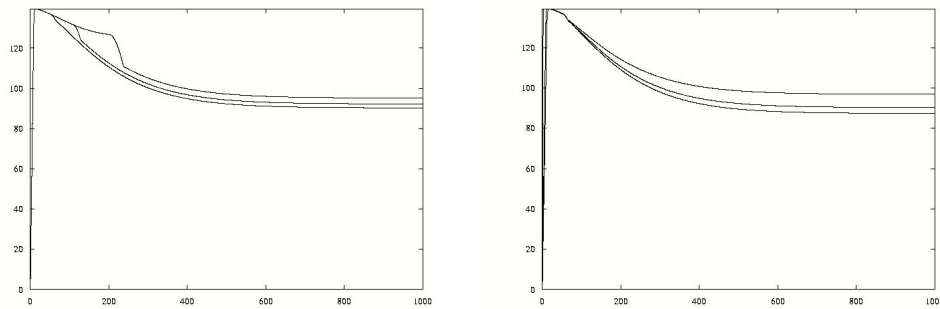


Fig. 23. *Left:* Trajectory of the internal copper in class BIR for different values of θ_B . Increasing θ_B produces an increase in the equilibrium of the internal copper. *Right:* Trajectory of the internal copper in class BIR for different values of k_s . Increasing k_s produces an increase in the equilibrium of the internal copper.